PERGAMON

Vision Research 39 (1999) 551–557

Vision Research

Shape and contour detection

Mark W. Pettet *

The Smith-Kettlewell Eye Research Institute, 2232 Webster Street, San Francisco, CA 94115, USA

Received 27 August 1997; received in revised form 19 December 1997

Abstract

Detectability of contours may be affected by long-range interactions between neurons in early stages of visual cortex. Specifically, neurons with receptive fields arrayed along the length of a contour may facilitate each other in a position- and orientation-dependent manner. Accordingly, the overall geometry of a contour should significantly influence both the strength of these long-range interactions and the contour's detectability. Psychophysical experiments measuring the detectability of sampled, curvilinear contours hidden by randomly-oriented and -positioned noise elements revealed two main findings. First, changes in direction of curvature degraded contour detectability. Second, the effect of changes in magnitude of curvature were predicted by the average of local curvature along the length of the contour. While the first result emphasizes the importance of uniform direction of curvature, the second result rules out penalties for deviation from circularity. © 1998 Elsevier Science Ltd. All rights reserved.

Keywords: Human; Psycophysics; Long-range interaction; Circular

1. Introduction

Visual processing of spatially extended contours may be mediated by long range facilitatory interactions between local orientation-selective units in early stages of visual cortex. Physiological studies suggest that the relative positions and the relative preferred orientations of interacting units are very important constraints on the strength of these facilitatory interactions (Rockland & Lund, 1982, 1983; Nelson & Frost, 1985; T'so, Gilbert & Wiesel, 1986; Kapadia, Ito, Gilbert & Westheimer, 1995; Weliky, Kandler, Fitzpatrick & Katz, 1995; Polat & Norcia, 1996; Bosking, Zhang, Schofield & Fitzpatrick, 1997). Moreover, facilitatory spatial interactions observed in psychophysical studies show positional and orientational dependencies consistent with this physiological architecture (Field, Hayes & Hess, 1993; Polat & Sagi, 1993, 1994). Therefore, if the detectability of a contour hidden in randomly-oriented noise is affected by such orientation- and position-dependent facilatatory interactions, then the overall geometry of a contour should have a significant effect on the strength of interactions between local units arrayed along its length. In other words, shape should affect detectability.

Some basic geometric constraints on detectability have already been worked out for sampled contours hidden in randomly oriented noise. For example, Field et al. (1993) presented groups of 12 Gabors aligned along a curvilinear contour path at regular intervals. These contour groups were hidden among several hundred randomly oriented and positioned Gabors. The detectabilty of the contour group was inversely related to the change in orientation from one element to the next along the contour path: i.e. straighter paths were more detectable. Also, when the individual elements' orientations deviated from alignment with the path, the detectability of the contour group also diminished. Field et al. (1993) explained their results with an 'association field' hypothesis, similar in many respects to several models of contour integration in the computer vision literature (Grossberg & Mingolla, 1985; Shashua & Ullman, 1988; Parent & Zucker, 1989; Kellman & Shipley, 1991; Nitzberg, Mumford & Shiota, 1991; Heitger & von der Heydt, 1993).

Subsequent studies by Kovacs and Julesz (1993) suggested that contour groups following closed circular paths were much more detectable than open-ended contours of similar curvature. However, sudden

* Tel.: +1 415 5611646; Fax: +1 415 5611610; e-mail: pettet@skivs.ski.org.

PII: S0042-6989(98)00130-8

changes in curvature (i.e. kinks) in a closed path caused diminished detectability compared to circular contours (Pettet, Mckee & Grzywacz, 1998). In the latter study, a computational simulation showed that the relative detectabilities of open-ended, closed (with kinks), and circular contours could be explained by lateral interactions like those proposed above. One important constraint used in the computer simulation was as follows. Given a fixed difference in orientation between two orientation-selective units, the degree of mutual facilitation was maximal when the two units were positioned so that their orientation axies were both tangeant to a circular path passing through their receptive field centers. In other words, interactions were strongest for circular contours. Although this constraint has some appealing computational aspects, it was also motivated by anecdotal reports from psychophysical observers that open-ended contours were easiest to see if they contained several neighboring elements falling along a common circular arc.

The studies presented here examined these various problems using a contour detection task similar to the one used by Field et al. (1993) to determine whether shapes that differed in their degree of circularity also differed in their detectability. In the context of this paper, 'the degree of circularity' indicates the extent to which a contour follows a path with no changes in direction or magnitude of curvature. Thus, two experiments were performed to test the relative effects of these two properties of circularity. The first experiment compared detectability of contours following circular paths to those following serpentine paths (i.e. constant local curvature with one or more changes in direction). The second experiment compared contours following circular and spiral (i.e. monotonic variation of curvature magnitude, no change in direction) paths. Together, these two experiments revealed how changes in path direction and changes in magnitude of curvature affected contour detectability.

2. Methods

2.1. Observers

The test subjects included the author and three other adults (one male and two females) naive to the purpose of the study. All had normal or corrected vision.

2.2. Stimuli

Stimulus patterns consisted of several dozen Gabor patch elements imaged on the screen of a 17 in. color monitor (Nanao) controlled by a microcomputer (Commodore) equipped with a high-speed graphics card (Merlin). Observers viewed the screen at a distance of 97 cm so that the pixel spacing in the 1024×768 viewing area subtended 1 arc min of visual angle. The overall dimensions of the viewing area at this observation distance were $17.0 \times 12.8°$.

Each Gabor patch was a 16×16 pixel bitmap whose pixel brightness values, L, at positions (x, y) relative to the center of the patch were scaled by the following formula:

$$L(x, y) = L_{\min} + L_{G}(L_{\max} - L_{\min}) + L_{\beta}$$

where

$L_{\min}$, minimum screen luminance (30 cd/m^2);
$L_{\max}$, maximum screen luminance (150 cd/m^2);
L_{β}, balancing factor (see below),

$$L_{G}(x, y) = \exp(-(x^2 + y^2)/2\sigma^2) \times \cos(2\pi x(x \sin\theta - y \cos\theta)/p),$$

where

σ, standard deviation of circularly-symmetric Gaussian envelope (4 arc min);
p, period of sinusoidal carrier (8 arc min);
θ, orientation of carrier.

By this definition, the orientation of the bright bar in the center of the Gabor patch was horizontal when $\theta = 0$, and the orientation rotated counter-clockwise as θ became more positive. The spatial frequency bandwidth of these Gabor patches was about 1.2 octaves, centered at 7.5 cd. The background luminance was set to $L_{\min} + (L_{\max} - L_{\min})/2$. The balancing factor, L_{β}, was added to make the measured mean luminance of the Gabor patches equal the background luminance. The balance of luminance between the Gabor patches and the background was confirmed by viewing the stimulus patterns from a distance of about 10 m. All luminances were measured with a Pritchard spectrophotometer.

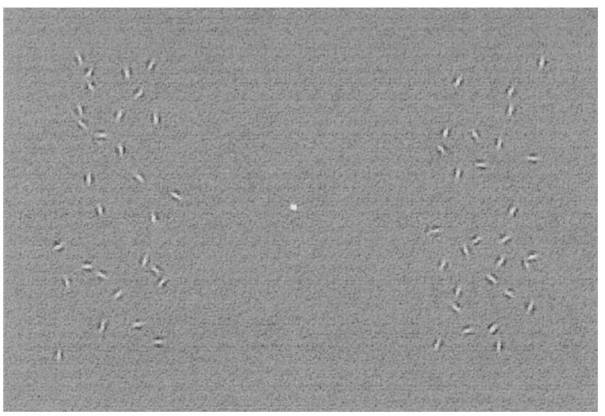

Fig. 1. Stimulus pattern. Observers were instructed to maintain fixation on the white dot, and to indicate whether the right or left element cluster contained a contour group. In the example shown here, the left cluster contains an instance of contour #4 (see Fig. 2A).

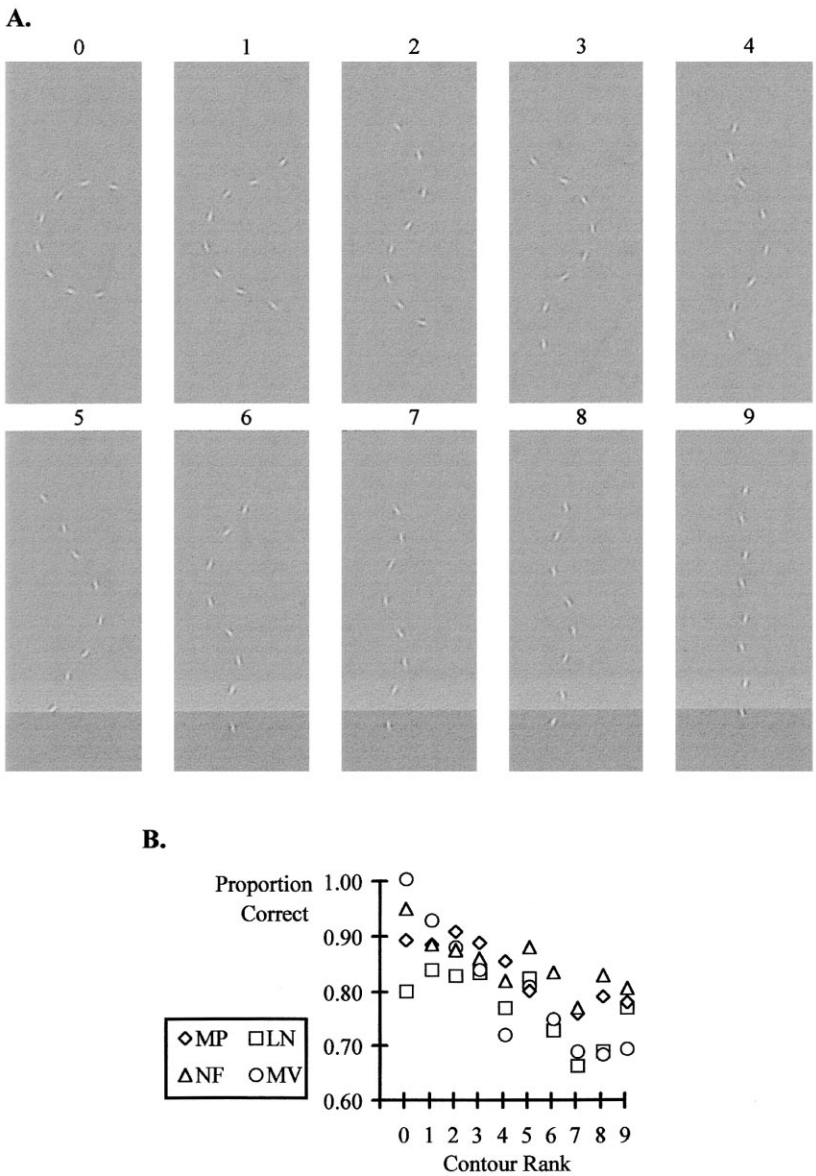

Fig. 2. Experiment 1: Effect of changes in direction of curvature. (A) The ten contour groups tested. The local curvature in the contour groups was fixed at $\pm 30°$, and the ten different contour shapes were generated by varying the frequency of changes in contour path direction. The identifying number assigned to each contour corresponded to the rank of the contour according to the circularity criteria described in the Section 3. (B) Performance of four observers.

Stimulus patterns were drawn by blitting Gabor patch bitmaps chosen from a library of 180 precalculated patches indexed by orientation in 1° increments. Positions and orientations of the elements in any given pattern were random, except that the individual Gabor patch bitmaps were non-overlapping.

Observers were shown two clusters of 30 Gabor patch elements[1]. The elements in each cluster had random orientations and random (non-overlapping) positions spread over $1.87 \times 4.67°$ areas centered 3° directly to the left and right of the fixation point (Fig. 1). In one of the clusters, several elements were arrayed along a spatially extended contour path. The elements in this contour group were evenly spaced apart by 40 arc min. The positions of immediate neighbors were constrained so their orientation axes were tangeant to a circular path fit through their centers.

Experiments 1 and 2 tested two different sets of contour groups. In Experiment 1, the contour groups consisted of eight elements. The difference in orientation between immediate neighbors (hereafter, local curvature) in the contour groups was fixed at $\pm 30°$. Ten different contour shapes ($\#0-\#9$ in Fig. 2A) were generated by varying the frequency of changes in contour path direction. Hence, each contour represented a

[1] Observer NF viewed clusters containing 25 Gabor patches each.

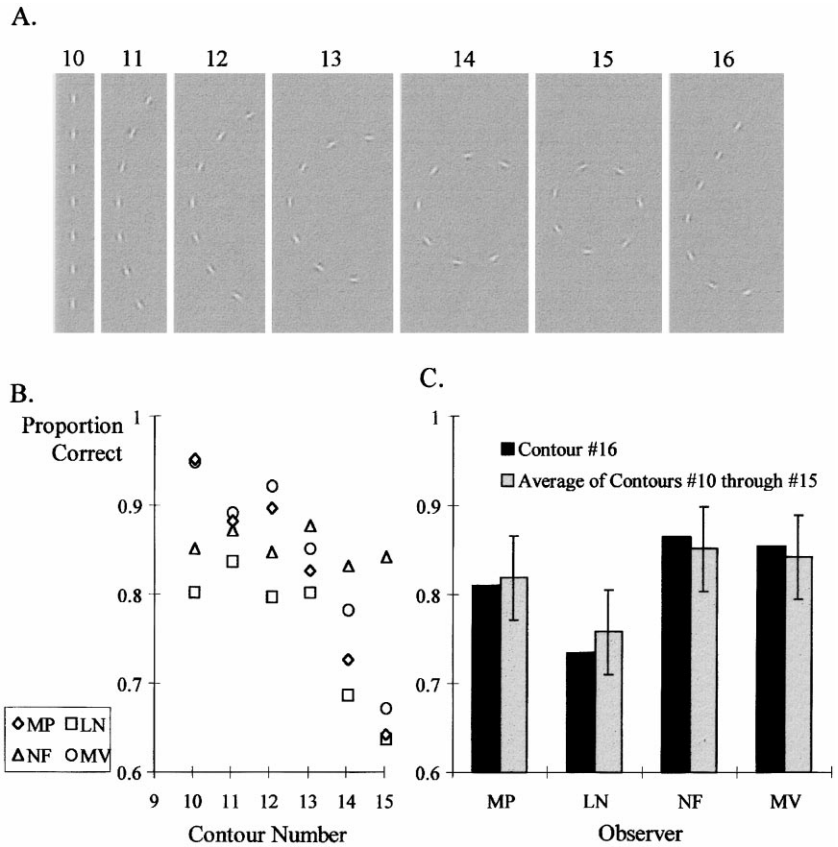

Fig. 3. Experiment 2: Effect of changes in magnitude of curvature. (A) The seven contour groups tested. The local curvature for the first six contours ranged from 0° for contour # 10 to 50° for contour # 15. The local curvature for contour # 16 increased monotonically from 0° for the first pair of elements to 50° for the last pair of elements. (B) Performance of four observers for contours # 10 through # 15. (C) Comparison of performance for contour # 16 to the average performance for contours in panel B. Note that the average of local curvatures for contours # 10– # 15 equals the average local curvature of contour # 16.

unique concatenation of circular arcs, all having the same magnitude of curvature, but alternating in direction. The contours ranged in shape from circular (i.e. no changes in path direction) to nearly straight (i.e. change in path direction after each element). In Experiment 2, the contour groups consisted of seven elements each. Six of the contour groups (# 10– # 15 in Fig. 3A) were circular arcs that differed in magnitude of local curvature. The local curvature ranged from 0° for contour # 10 to 50° for contour # 15. Contour # 16 followed a spiral path so that the local curvature increased from 0 to 50° along the length of the contour. The average local curvature in contour # 16 equalled the average of the local curvatures for contours # 10 through # 15.

Some contour groups spanned considerable retinal distances (e.g. contour # 7 was 4.67° in length). Thus, to minimize changes in retinal eccentricity along their length, the overall orientation of the contours were constrained so that their axes of least second moment (i.e. their 'long axes') were vertical. The contour group assumed a random position within the bounds of the target cluster. On each trial, the chosen contour was randomly flipped vertically or reflected horizontally, or both.

The stimulus configuration described here represents a departure from conventional stimuli in which a contour group can appear anywhere, in any orientation, within a large field of many random Gabor patches (Field et al., 1993). The use of this new configuration was motivated by several considerations. First, pilot studies (data not shown) indicated that differences in contour detectability due to differences in shape were very slight. Thus, every confounding source of variability in the data had to be removed to maximize the sensitivity of the technique. Positional uncertainty of contour location was considered to be a large source of variability for two reasons. First, if the contour was allowed to fall anywhere within a large area, then the eccentricity of the contour would vary from trial to trial. Pilot data (not shown) again suggested that contour detectability diminished significantly with eccentricity (Hess & Dakin, 1997). Thus, variability in eccentricity would lead to variability in detectability. Second, if the contour was allowed to fall anywhere within a large area, the observer, in effect, would be

performing a search task. When the search area is large, significant trial-to-trial changes in search strategy may occur. Again, this may lead to changes in performance. The stimulus configuration employed in the current study reduces both of these effects by holding eccentricity constant and minimizing the search area. The choice of 3° eccentricity for the noise clusters was also based on the results from the eccentricity pilot data. At eccentricities nearer fixation, observers achieved near perfect performance, thus obscuring differences between the various contours tested. The opposite effect occurred at more distant eccentricities: performance was near chance levels for most of the different contours.

2.3. Procedure

Each trial began with a blank screen containing a small white fixation dot at the center. A button press initiated the stimulus presentation, which lasted for 150 ms. Observers were instructed to maintain fixation on the white dot, and indicate by pressing one of two buttons whether the right or left element cluster contained the contour group. Once the forced-choice response was recorded, the next stimulus presentation was initiated.Stimuli were presented in sequences of 100 trials (Experiment 1) or 70 trials (Experiment 2), with different contours selected at random for each trial. An experimental session consisted of several of these sequences seperated by 1–2 min rest periods. Each data point in Figs. 2 and 3 represents a total of 200 responses, collected from at least two sessions on seperate days.

3. Results

To evaluate trends in performance caused by changes in contour path direction, the contours in Experiment 1 were ranked and assigned identifying numbers (see Fig. 2A) according to the length of the longest circular arc in each contour path. For example, contour #3, whose longest circular arc contained five elements, was given a higher rank than contour #5, whose longest circular arc contained four elements. When two contours had the same number of elements in their longest circular arc (e.g. contours #4 and #5), they were ranked according to the length of their second-longest circular arc. Thus, according to this scheme, contour #0, which followed a single circular arc along its entire length, was given the highest rank, while contour #9, which had no arcs greater than two elements, was given the lowest rank.

In Fig. 2B, performance in the detection task was plotted against the rank of contours. Single factor, within-subject ANOVA (d.f. = 9, 190) showed significant ($P < 0.05$) differences between the ten contour shapes for all observers. In general, the proportion of correct responses was larger for higher-ranked contours. To rule out cues generated by the positional arrangement or local density of contour elements, control stimuli were presented in which the orientations of the individual contour elements were randomized. The relative positions of the elements in each contour group, and the overall orientation of the contour were the same as in the previous experiment. Performance was at chance levels for all the control contours (data not shown), and ANOVA showed no significant difference between the ten control contour shapes for any observer. This result verifies that detection of the contour group required orientational alignment of elements along the contour path.

According to results of Experiment 1, contours following circular paths were more detectable than contours that follow paths with changes in direction. Experiment 2 examined how changes in magnitude of curvature affected contour detectability by testing the following hypothesis. If contour detection mechanisms are truly selective for circular contours, then changes in magnitude of curvature along a contour path might invoke some kind of penalty that suppresses detectability. Demonstrating such a penalty was complicated by the fact that contour detectability decreases with increasing path curvature (Field et al., 1993). For example, in the case of the spiral contour used in Experiment 2 (Fig. 3A, #16), the outermost segment of the spiral with low curvature was more detectable than the innermost segment with high curvature. Therefore, to estimate any additional penalty incurred by changes in curvature along the spiral, an expectation value was derived for the detectability of the spiral based on the average detectability of the various segments comprising the spiral. The detectability for a given segment of the spiral was estimated by measuring the detectability of a circular contour of equivalent curvature. Hence, the overall expectation value for the spiral contour's detectability was simply the average detectability of a series of circular contours (Fig. 3A, #10–#15) whose curvatures respectively equalled the local curvature of each segment of the spiral contour (#16). If any penalty exists, then the performance for contour #16 should be significantly lower than the average performance for contours #10–#15.

Performance for contours with varying magnitude of curvature (Experiment 2) is plotted in Fig. 3B. For contours #10–#15, the proportion of correct responses remained high for curvatures up to about 30° (contour #13). At higher curvatures, performace dropped significantly for three observers. Observer NF's performance was roughly constant for all six contours. In Fig. 3C, proportion of correct responses for contour #16 (filled bars) is compared to the aver-

age proportion of correct responses for contours # 10 through # 15 (open bars). There was no significant difference between these two quantities for any of the observers. Thus, there was no evidence for an additional penalty for changes in curvature.

4. Discussion

Because of considerable variation between observers, it was difficult to draw conclusions about the relative discriminability of the various shapes tested in Experiment 1. However, one qualitative trend seemed consistent. For each observer, the contours with extended circular arcs (# 0– # 3) were easier to detect than the contours with multiple changes in direction (# 7– # 9). However, this principle only held for the most extreme examples. For example, contour # 3 contained a five-element circular arc, while contour # 5 contained a four-element circular arc. Nevertheless, observer NF performed better with contour # 5 than contour # 3. More generally, when comparing contours with very similar overall shapes, no consistent pattern of relative detectability held for all four observers. It is likely that trial-to-trial variability in the configuration of the two random element clusters concealed fine differences in contour detectability.

In Experiment 2, high curvature impaired detectability of the circular contours relative to straight contours. Field et al. (1993), (Fig. 7) reported a similar trend. Furthermore, the equivalence between the detectability of the spiral contour (# 16) and the average detectability of the circular contours (# 10– # 15) rules out additional penalties for changes in magnitude of curvature. In other words, the detectability of a contour with a monotonic change in curvature magnitude can be predicted by the average (or some other cumulative estimate) of local curvature along its length.

One curious finding concerned the difference in detectability of comparable contours in Experiments 1 and 2. Specifically, contour # 0 was much easier to detect than contour # 14 (averages of 91 and 76% correct responses, respectively). Although contour # 0 has one more element than contour # 14, this difference in length does not account for the difference in visibility (Kovacs & Julesz, 1993). This discrepancy might be explained by the procedure used to collect the data. In each experiment, the contour presented on each trial was selected at random from the full set of contours used in that experiment. Since the set of contours presented in Experiment 1 differed from those in Experiment 2, observers may have employed different strategies to perform the task in the two experiments. For example, observers may have preferentially looked for the most detectable contours in each of the two sets. While such an approach may have degraded performance for the non-preferred contours, enhanced detection of the preferred contours may have led to a net increase in overall performance. According to this reasoning, since contour # 0 was the most visible member of the set for Experiment 1, and contour # 14 was nearly the least visible memeber of the set for Experiment 2, the performance for contour # 14 would be degraded relative to contour # 0. In any case, whatever the explanation for the discrepancy, none of the conclusions of this study relied on comparisons of performance between contours presented in the two different experiments.

In summary, two important results are clear. First, when the local curvature of a contour is held constant, changes in direction of curvature degrade detectability. Second, when the direction of curvature of a contour is held constant, increased curvature degrades detectability, but changes in magnitude of curvature along the length of a contour have no additional effect.

Circularity is an important property that may constrain long range faciltatory interactions between localized, orientation-selective spatial filtering mechanisms. In fact, ring-shaped receptive fields have been reported in extra-striate cortex (Gallant, Connor, Rakshit, Lewis & Van Essen, 1996), and have been proposed as a mechanism for curvature discrimination (Wilson & Wilkinson, 1996). Furthermore, oriented line elements following a circular path can be fit with curves having no changes in curvature. Such structural regularity may be just enough of a cue to bolster the signal associated with a spatially extended contour so that it becomes more detectable in the presence of confounding information generated by surface textures. Hence, the co-circularity constraint occurs in some computational models of contour integration (Parent & Zucker, 1989; Yen & Finkel, 1996). However, while effective contour integration does require uniform direction of curvature (Experiment 1), it does not require circularity per se (Experiment 2). Of course, the latter finding does not exclude detection of spiral contours by a combination of processing modules sensitive to circular contours. Rather, it suggests that selectivity for circular contours is not maintained by active suppression of non-circular contours.

Whatever the specific geometric constraints, long range interaction between spatially dispersed pattern elements provides an attractive model for binding together the discrete neural signals generated by a spatially extended contour. Although direct physiological evidence is still scant, the importance of collinearity for such interactions has already been established (Nelson & Frost, 1985; Kapadia et al., 1995; Bosking et al., 1997). It will be interesting to see whether co-circularity will also be as important. Although such mechanisms are far removed from explaining the finer points of shape detection and discrimination, they certainly help

in establishing the sequence of events leading to a complete neural representation of complex visual shapes.

Acknowledgements

Supported by NIH EY06672-01, AFOSR F49620-95-1-0265, and by a Rachael C. Atkinson Fellowship for Eye Research. Thanks to Suzanne McKee for sponsorship of this research program.

References

Bosking, W. H., Zhang, Y., Schofield, B., & Fitzpatrick, D. (1997). Orientation selectivity and the arrangement of horizontal connections in tree shrew striate cortex. *Journal of Neuroscience*, *17*(6), 2112–2127.

Field, D. J., Hayes, A., & Hess, R. F. (1993). Contour integration by the human visual system: evidence for a local 'association field.'. *Vision Research*, *33*(2), 173–193.

Gallant, J. L., Connor, C. E., Rakshit, S., Lewis, J. W., & Van Essen, D. C. (1996). Neural responses to polar, hyperbolic, and Cartesian gratings in area V4 of the macaque monkey. *Journal of Neurophysiology*, *76*, 2718–2739.

Grossberg, S., & Mingolla, E. (1985). Neural dynamics of form perception: boundary completion, illusory figures, and neon color spreading. *Psychology Review*, *92*, 173–211.

Heitger, F., von der Heydt, R. (1993). A computational model of neural contour processing: figure-ground segregation and illusory contours. *Proceedings of the International Conference on Computer Vision*, 32–40.

Hess, R. F., & Dakin, S. C. (1997). Absence of contour linking in peripheral vision. *Nature*, *390*, 602–604.

Kapadia, M. K., Ito, M., Gilbert, C. D., & Westheimer, G. (1995). Improvement in visual sensitivity by changes in local context: parallel studies in human observers and in V1 of alert monkeys. *Neuron*, *15*, 843–856.

Kellman, P. J., & Shipley, T. F. (1991). A theory of visual interpolation in object perception. *Cognitive Psychology*, *23*, 141–221.

Kovacs, I., & Julesz, B. (1993)). A closed curve is much more than an incomplete one: effect of closure in figure-ground segmentation. *Proceedings of the National Academy of Science*, *90*, 7495–7497.

Nelson, J. I., & Frost, B. J. (1985). Intracortical facilitation among co-oriented, co-axially aligned simple cells in cat striate cortex. *Experimental Brain Research*, *61*(1), 54–61.

Nitzberg, M., Mumford, D., & Shiota, T. (1991). *Filtering, segmentation, and depth*. Berlin: Springer-Verlag.

Parent, P., & Zucker, S. W. (1989). Trace inference, curvature consistency, and curve detection. *IEEE Transactions on Pattern Analaysis and Machine Intelligence*, *11*, 823–839.

Pettet, M. W., Mckee, S. P., & Grzywacz, N. M. (1998). Smoothness constrains long range interactions mediating contour detection. *Vision Research*, *38*, 865–879.

Polat, U., & Norcia, A. M. (1996). Neurophysiological evidence for contrast dependent long range facilitation and suppression in the human visual cortex. *Vision Research*, *36*, 2019–2099.

Polat, U., & Sagi, D. (1993). Lateral interactions between spatial channels: suppression and facilitation revealed by lateral masking experiments. *Vision Research*, *33*(7), 993–999.

Polat, U., & Sagi, D. (1994). The architecture of perceptual spatial interactions. *Vision Research*, *34*(1), 73–78.

Rockland, K. S., & Lund, J. S. (1982). Widespread periodic intrinsic connections in the tree shrew visual cortex. *Brain Research*, *169*, 19–40.

Rockland, K. S., & Lund, J. S. (1983). Intrinsic laminar lattice connections in primate visual cortex. *Journal of Comparative Neurology*, *216*, 303–318.

Shashua, A., Ullman, S. (1988). Structural saliency: the detection of globally salient structures using a locally connected network. *Proceedings of the International Conference on Computer Vision*, 321–327.

T'so, D. Y., Gilbert, C. D., & Wiesel, T. N. (1986). Relationships between horizontal interactions and functional architecture in cat striate cortex as revealed by cross-correlation analysis. *Journal of Neuroscience*, *6*, 1160–1170.

Weliky, M., Kandler, K., Fitzpatrick, D., & Katz, L. C. (1995). Patterns of excitation and inhibition evoked by horizontal connections in visual cortex share a common relationship to orientation columns. *Neuron*, *15*, 541–552.

Wilson, H. R., & Wilkinson, F. (1996). Non-Fourier mechanisms in human form vision: psychophysical data and theory. *Investigative Ophthalmology and Visual Science Supplement*, *37*, 955.

Yen, S., & Finkel, L. H. (1996). 'Pop-out' of salient contours in a network based on striate cortical connectivity. *Investigative Ophthalmology and Visual Science Supplement*, *37*, 293.